

Relationships between ground and aerial photography and geothermal vegetation at Craters of the Moon geothermal area, Waikato

Prepared by:
Kelvin Lloyd, Des Smith, Chris Bycroft, Steve Rate
(Wildlands)

For:
Waikato Regional Council
Private Bag 3038
Waikato Mail Centre
HAMILTON 3240

August 2016

Document #: 9335872

Peer reviewed by:
Katherine Luketina

Date July 2017

Approved for release by:
Mike Scarsbrook

Date March 2019

Disclaimer

This technical report has been prepared for the use of Waikato Regional Council as a reference document and as such does not constitute Council's policy.

Council requests that if excerpts or inferences are drawn from this document for further use by individuals or organisations, due care should be taken to ensure that the appropriate context has been preserved, and is accurately reflected and referenced in any subsequent spoken or written communication.

While Waikato Regional Council has exercised all reasonable skill and care in controlling the contents of this report, Council accepts no liability in contract, tort or otherwise, for any loss, damage, injury or expense (whether direct, indirect or consequential) arising out of the provision of this information or its use by you or any other party.

**RELATIONSHIPS BETWEEN GROUND AND
AERIAL PHOTOGRAPHY AND GEOTHERMAL
VEGETATION AT CRATERS OF THE
MOON GEOTHERMAL AREA, WAIKATO**



 providing
outstanding
ecological
services to
sustain
and improve our
environments



RELATIONSHIPS BETWEEN GROUND AND AERIAL PHOTOGRAPHY AND GEOTHERMAL VEGETATION AT CRATERS OF THE MOON GEOTHERMAL AREA, WAIKATO

Contract Report No. 4010

August 2016

Project Team:

Kelvin Lloyd - Report author

Des Smith - Statistical analysis, report author

Roger Bawden - GIS applications

Chris Bycroft - Field work, report author

Steve Rate - Report author

Sarah Beadel - Project manager, field work, report author, peer review

Mark Harvey (Harvey Geoscience) - Drone capture of imagery

Prepared for:

Waikato Regional Council

Private Bag 3038

Waikato Mail Centre

Hamilton 3240

EXECUTIVE SUMMARY

Near-infrared (NIR) imagery has been used elsewhere to detect stressed vegetation, and could be used to automate detection of changes in the stress levels experienced by geothermal vegetation, e.g. those caused by changes in heat flow. NIR contains wavelengths that are used to calculate Normalised Difference Vegetation Index (NDVI). Recent drone-captured imagery at Craters of the Moon area, Wairakei, New Zealand, including RGB (normal colour aerial imagery), near infrared (NIR), and thermal infrared (TIR), was used to generate NDVI values and investigate their use in assessing stressed geothermal vegetation. By assessing geothermal vegetation stress on the ground, and relating it to NDVI by taking downward-focused NIR images of geothermal vegetation, the potential link between NDVI and vegetation stress was examined in geothermal vegetation, with a view to investigating the relationship between changes in heat flow and vegetation stress. Stressed geothermal vegetation (identified subjectively through percentage cover of dead foliage), and in particular vegetation dominated by geothermal kānuka, can be identified by ground-based NDVI values at a relatively small scale. Aerial TIR had a surprisingly poor relationship with geothermal kānuka dieback or stature, and was also poorly related to ground-based NDVI.

CONTENTS

EXECUTIVE SUMMARY

1.	INTRODUCTION	1
2.	SITE DESCRIPTION	1
3.	METHODS	2
3.1	Review of information	2
3.2	Aerial photography with drone	2
3.3	Ground-based photography	3
3.4	Analysis of photography	3
3.4.1	Terrestrial based NDVI calculations	3
3.4.2	Terrestrial based NDVI analysis	5
3.4.3	Aerial based NDVI analysis	5
3.4.4	Analysis of aerial-based TIR versus NDVI	6
3.4.5	Photopoint analysis of Aerial based TIR versus NDVI	8
3.5	Statistical analyses	8
4.	STRESS AND GEOTHERMAL VEGETATION	8
5.	NORMALISED DIFFERENCE VEGETATION INDEX (NDVI)	8
5.1	Overview	8
5.2	Limitations of NDVI	9
5.3	NDVI values used to assess vegetation	10
6.	RESULTS	10
6.1	Ground-based NDVI analyses	11
6.1.1	Ground-based NDVI and vegetation dieback	11
6.1.2	Ground-based NDVI and vegetation height	12
6.1.1	Ground-based NDVI and habitat type	12
6.2	Aerial TIR and NDVI analyses	15
6.2.1	Aerial TIR versus aerial NDVI in geothermal kanuka	15
6.2.2	Aerial TIR versus aerial NDVI for geothermal habitats	16
6.2.1	Aerial TIR versus geothermal stress and ground-based NDVI	16
6.3	Soil temperature and geothermal vegetation stress	17
6.3.1	Soil temperature and geothermal kākūka dieback	17
6.3.2	Soil temperature and geothermal kākūka height	18
7.	DISCUSSION	19
8.	CONCLUSIONS	20
	ACKNOWLEDGMENTS	21
	REFERENCES	21
	APPENDIX	
1.	Ground-based vertical RGB and NIR photographs	23

Reviewed and approved for release by:



Sarah Beadel
Director
Wildland Consultants Ltd

© *Wildland Consultants Ltd* 2016

This report has been produced by Wildland Consultants Ltd for Waikato Regional Council. Wildland Consultants accepts no responsibility for any use of, or reliance on any contents of this Report by any person other than Waikato Regional Council. This information may be copied or redistributed to others without limitation, provided Wildland Consultants Ltd is acknowledged as the source of information.

1. INTRODUCTION

Waikato Regional Council contracts five-yearly capture of Red, Green and Blue (RGB) and Near Infra-Red (NIR) imagery over geothermal sites, and routinely uses the RGB imagery to help map geothermal vegetation and habitats and determine whether any changes have taken place. NIR imagery has been used elsewhere to detect stressed vegetation (Weier and Herring 2000, U.S. Geological Survey 2015), and potentially could be used to detect changes in the stress levels experienced by geothermal vegetation, for example those caused by changes in heat flow. NIR contains bands of imagery that are used to calculate Normalised Difference Vegetation Index (NDVI), so can be used to generate NDVI values for geothermal areas. NDVI has been widely calculated from satellite imagery to determine the density of green vegetation, and areas of stressed and unstressed vegetation, at a sub-continental scale.

Waikato Regional Council has also recently commissioned capture of aerial data by uncrewed aerial vehicles (UAV), commonly referred to as drones, over geothermal areas. Drone-captured data is potentially ideal for geothermal sites, as health and safety issues often prevent full access for ground-based measurement and description. Drone-captured imagery can help to determine the boundaries of geothermal sites, and different kinds of vegetation and habitat within geothermal sites, and currently unknown geothermal sites. Recent drone-captured imagery includes RGB (normal colour aerial imagery), near infrared (NIR), and thermal infrared (TIR), and thus can also be used to generate NDVI values and potentially assess stressed vegetation.

The purpose of this trial was to investigate whether drone-captured aerial photography can be used to determine the degree of stress exhibited by thermophilic terrestrial ecosystems. By assessing geothermal vegetation stress on the ground, and relating it to NDVI by taking downward-focussed NIR images of geothermal vegetation, the potential link between NDVI and vegetation stress can be examined in geothermal vegetation. If vegetation stress is also related to TIR imagery from the drone-flown data, then the relationship between heat flow and vegetation stress can also be determined. If these links are demonstrated, then the regular five-yearly aerial capture of NIR could be used to determine geothermal vegetation stress caused by changes in geothermal activity, including heat flow or fluid discharge chemistry.

2. SITE DESCRIPTION

The Craters of the Moon site was selected for assessment due to its variety of geothermal habitat types, thermal environments, and relatively safe access to a range of thermal environments for ground-based photography. Vegetation at the site includes a variety of geothermal kānuka (*Kunzea tenuicaulis*) scrub shrubland types, and mixed scrub and shrublands of other species, as well as small areas of fernland and mossfield (Wildland Consultants 2014). The site is large and in good condition. Commissioning of the nearby Wairakei geothermal power station resulted in an overall increase in geothermal activity at Craters of the Moon, which has resulted in increases in the extent of geothermal vegetation at the site. Changes in geothermal activity are ongoing, which adds to the value of the pilot project at the site, which will provide a baseline assessment against which future changes can be assessed. This site

provides a testing ground for developing the technology and processes for detecting changes.

3. METHODS

3.1 Review of information

Relevant information addressing use of NDVI data was reviewed. This information included scientific articles, reports, and information on websites.

3.2 Aerial photography with drone

Imagery was collected using a modified DJI Phantom 2 Vision plus quadcopter (Figure 1). The quadcopter was modified by the replacement of the stock camera with an ICI 640x480 uncooled thermal sensor (spectral response 7-14 μ m) with automated image capture (ICI UAV module[®]), (Harvey *et al.*, 2016). A Canon Powershot S100 point and shoot camera was fitted for normal red, green and blue (RGB) output. A modified Canon Powershot SX260 point and shoot camera was fitted for near infrared, green and blue (NGB) output. The SX260 was modified by addition of a glass filter to remove red light, and allow collection of near infrared light. All camera systems automatically geotag images which provides georeferenced output.



Figure 1: DJI Phantom 2 Vision Plus quadcopter modified with ICI thermal camera and UAV module.

An appropriate flight plan was determined using UgCS[®] software running on a Hewlett Packard laptop running Windows 7[®]. The flight plan was then uploaded to the quadcopter's flight controller via a Samsung S4 smartphone running Android and the UgCS[®] mobile companion App. Accordingly, both in-flight navigation and image capture were autonomous.

For thermal imagery, four flights were made between 0600 and 0800 on 2 April 2016. Flight conditions were clear and cool (12°C) in the early morning, with light winds *c.* 1 m/s. For RGB and NIR imagery, four flights were made between 1100 and 1400

on 28 April 2016. Flight conditions were clear and sunny (16°C), with light winds c.1 m/s. All flights were made at 120 m altitude above ground, at a speed of c.8 m/s.

3.3 Ground-based photography

Selected areas of the Craters of the Moon site were visited on two occasions: 9 May 2016 (1357 to 1549 hours) and 2 June 2016 (1020 to 1350 hours). During these periods, weather was similar to that experienced during the drone photography (sunny conditions with few clouds) earlier in the season. The same cameras and settings used for drone photography were used for ground based photographs: RGB (Canon Powershot S100) and NGB (Canon Powershot SX260 HS). All photographs were taken in sunshine. On 2 June, some waiting time was required between passing clouds to take photographs.

Photographs were taken of geothermal kānuka in a range of height and dieback conditions, as well as selected examples of other vegetation and habitats present at Craters of the Moon, including *Campylopus* mossfield, bracken (*Pteridium esculentum*) fernland, mingimingi (*Leucopogon fasciculatus*) scrub, a cotoneaster (*Cotoneaster glaucophyllus*) shrub, *Lycopodiella cernua* fernland, and bare ground (Figure 2). Photographs were taken vertically downward, attempting to avoid capturing the photographer's footwear in the frame.

The following information was also collected for each vertical photograph site:

- GPS location
- Vegetation description
- Height of vegetation
- Percent of key vegetation and habitat types present, including non-vascular plant cover, bare ground and litter.
- Percent cover of dieback of woody vegetation.
- Soil temperatures at 2 cm, 15 cm, and 40 cm depth.

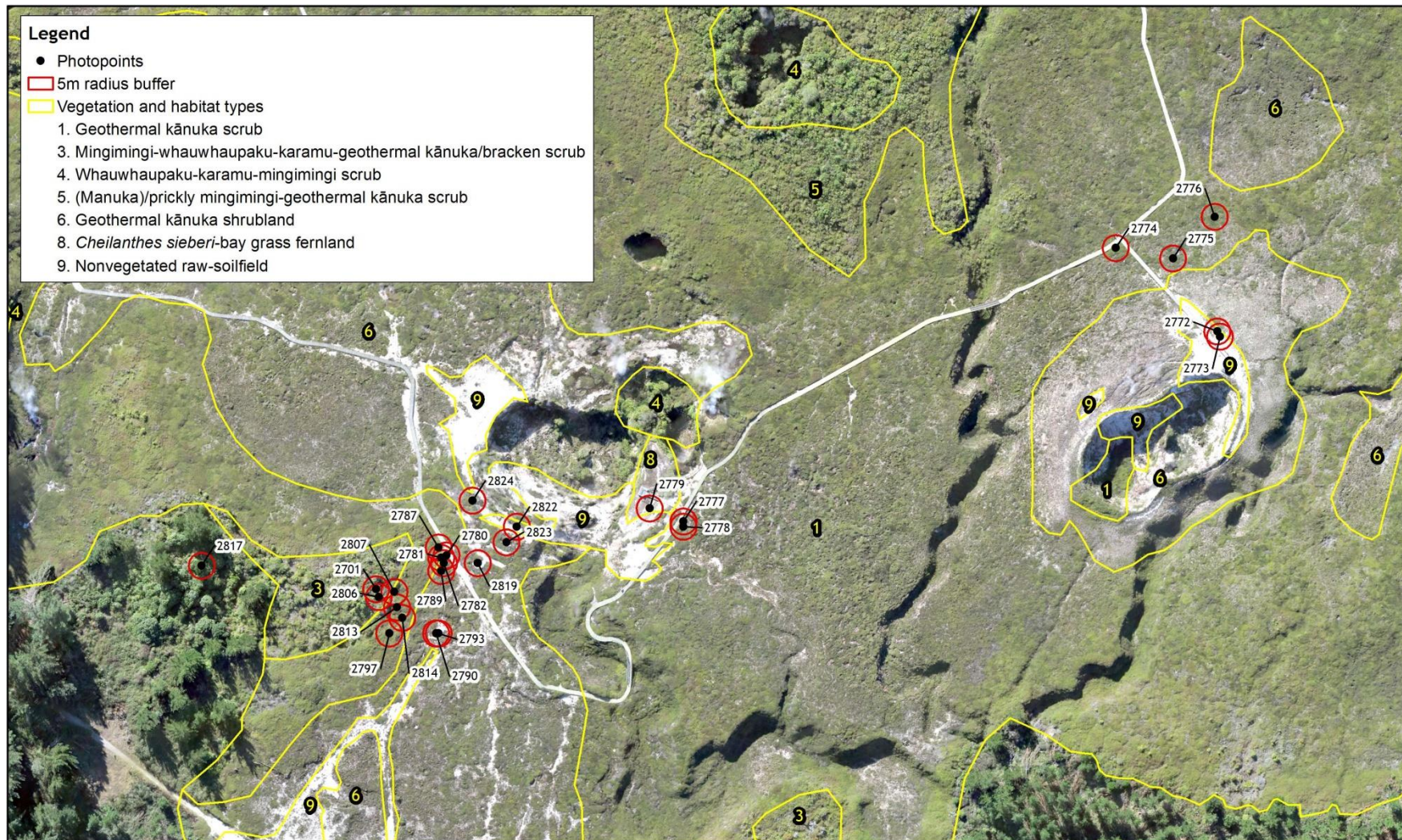
3.4 Analysis of photography

In our analysis, the inputs for NDVI are an image with a NIR band (mapped to red), green band and blue band, with the output being a new image file/layer of NDVI. This conversion was done in ArcGIS. Further details are below.

3.4.1 Terrestrial based NDVI calculations

NDVI was calculated for each NIR image with the QGIS Raster Calculator tool using the formula supplied by Harvey Geoscience $BNDVI = (NIR - BLUE) / (NIR + BLUE)$. All images were exported as TIF files for further image analysis.

The calculated ground based NDVI data was reclassified in ArcGIS using the 'Reclassify' tool (Table 1).



- Legend**
- Photopoints
 - 5m radius buffer
 - Vegetation and habitat types
 - 1. Geothermal kānuka scrub
 - 3. Mingimingi-whauwhaupaku-karamu-geothermal kānuka/bracken scrub
 - 4. Whauwhaupaku-karamu-mingimingi scrub
 - 5. (Manuka)/prickly mingimingi-geothermal kānuka scrub
 - 6. Geothermal kānuka shrubland
 - 8. *Cheilanthes sieberi*-bay grass fernland
 - 9. Nonvegetated raw-soilfield

Data Acknowledgment

Map contains data sourced from LINZ
Crown Copyright Reserved

Report: R4010
Client: ENVIWAIK
Ref: 01 1698
Path: E:\gis\EW_Geothermal_Sites_2003\UAV_data\mxd\
File: Craters_photopoints_withbuffers.mxd

Figure 2. Ground-based photography sites, Craters of the Moon Geothermal Area



Wildlands © 2016
www.wildlands.co.nz, 0508 WILDNZ

Scale: 1:2,000
Date: 11/08/2016
Cartographer: RPB
Format: A4R

Table 1: Reclassification of NDVI values.

Low Value	High Value	Reclassified Value
-1	0	1
0	0.01	2
0.01	0.02	3
0.02	0.03	4
0.03	0.04	5
0.04	0.05	6
0.05	0.06	7
0.06	0.07	8
0.07	0.08	9
0.08	0.09	10
0.09	0.1	11
0.1	0.11	12
0.11	0.12	13
0.12	0.13	14
0.13	0.14	15
0.14	0.15	16
0.15	0.16	17
0.16	0.17	18
0.17	0.18	19
0.18	0.19	20
0.19	0.2	21
0.2	0.21	22
0.21	0.22	23
0.22	0.23	24
0.23	0.24	25
0.24	0.25	26
0.25	0.3	27
0.3	1	28

3.4.2 Terrestrial based NDVI analysis

Any parts of the data that had human interference (legs, shoes, or equipment) was set to NULL so that it didn't interfere with calculations. The number of cells within each reclassified value was then exported to Microsoft Excel for analysis. The reclassified data was also exported as an image for visual interpretation. All data was also exported to ASCII format for analysis in R. This data was in the form of rows and columns based on the original dataset.

3.4.3 Aerial based NDVI analysis

Small areas of known vegetation, plants, and substrate type were mapped onto the RGB imagery to explore their NDVI signatures (Table 2; Figure 3). Different areas were sampled for different substrates to avoid shadow effects and avoid capture of other substrate types). These substrate types include non-living substrates such as asphalt, boardwalk, buildings, vehicles, tracks, and a wooden bridge, and various vegetation types, habitats, and plant species, including different-statured stands of geothermal kānuka, mixed shrubland, exotic grassland, mown grassland, soil, mossfield, pine plantations, felled pine trees, bracken, cotoneaster, eucalyptus (*Eucalyptus* sp.), and rock fern (*Cheilanthes sieberi*). These small areas of each substrate type were then run through ArcGIS 'Zonal Statistics to Table' to calculate

Count, Min, Max, Range, Mean, Standard Deviation and Sum for the cells falling within the polygon. These data were then exported to Microsoft Excel for summary and analysis.

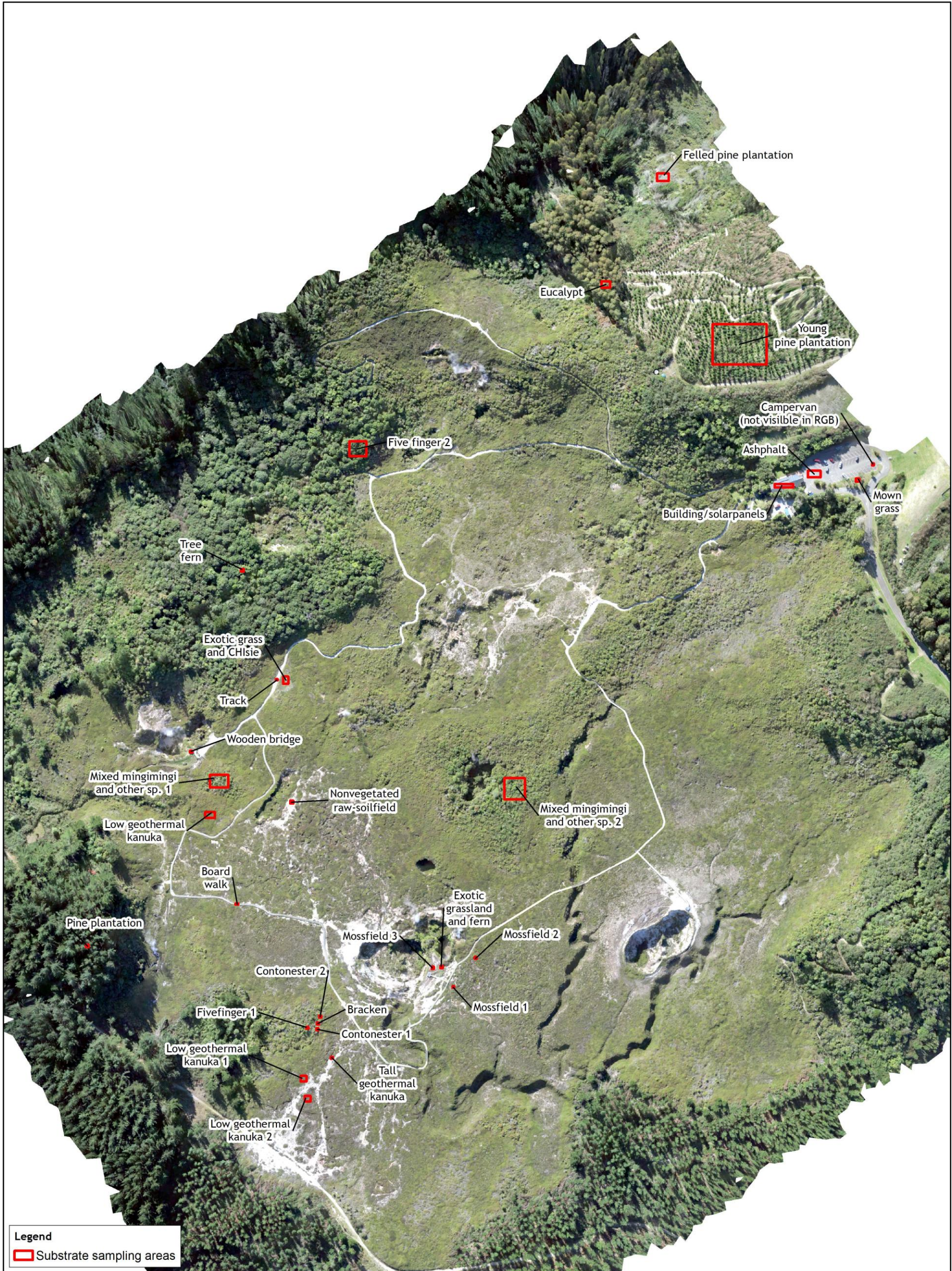
While NDVI values for different substrates have large ranges, mean NDVI values have low standard errors (all ± 0.0008 or less). The most prominent feature of the NDVI values of these substrates is that non-living substrates have negative mean NDVI values, and live vegetation has positive mean NDVI values (Table 2). Within live vegetation, indigenous and exotic trees and shrubs generally have higher (>0.08) mean NDVI values, while geothermal grassland, fernland, and mossfield have low (<0.05) mean NDVI values (Table 2).

Table 2: NDVI values for a range of vegetation, plants, and substrates.

VegetationSubstrate Type	Minimum NDVI	Maximum NDVI	Mean NDVI	Median NDVI
Pine	0.007	0.158	0.094	0.095
Young pines	-0.076	0.197	0.086	0.092
Eucalyptus	-0.035	0.200	0.087	0.082
Tree ferns	0.038	0.154	0.089	0.089
Whauwhaupaku 1	0.067	0.147	0.110	0.108
Whauwhaupaku 2	-0.039	0.206	0.096	0.092
Cotoneaster 1	0.000	0.175	0.110	0.114
Mixed mingimingi shrubland 1	-0.116	0.233	0.094	0.092
Mixed mingimingi shrubland 1	-0.098	0.217	0.087	0.095
Geothermal kānuka (low)	0.038	0.157	0.098	0.097
Geothermal kānuka (low)	0.038	0.134	0.081	0.086
Geothermal kānuka (low)	-0.004	0.120	0.028	0.039
Geothermal kānuka (tall)	-0.059	0.106	0.069	0.072
Bracken	-0.050	0.102	0.041	0.044
Grass/fernland(<i>Cheilanthes</i>)	-0.065	0.128	0.038	0.045
Grass/fernland (other ferns)	-0.061	0.076	0.036	0.036
Mown grass 1	-0.010	0.091	0.035	0.033
Mown grass 2	0.078	0.121	0.096	0.110
Mossfield 1	0.020	0.093	0.045	0.045
Mossfield 2	-0.040	0.059	0.017	0.013
Mossfield 3	-0.027	0.049	0.006	0.000
Felled pines	-0.067	0.087	-0.003	-0.010
Geothermal bare ground	-0.094	0.012	-0.037	-0.027
Other Features				
Track	-0.174	-0.088	-0.148	-0.149
Boardwalk	-0.168	-0.101	-0.132	
Building	-1.000	-0.017	-0.202	-0.169
Campervan	-0.381	0.008	-0.064	-0.061
Asphalt	-0.200	-0.119	-0.155	-0.149
Wooden bridge	-0.198	-0.039	-0.121	-0.117

3.4.4 Analysis of aerial-based TIR versus NDVI

Ten thousand random points were created in ArcGIS throughout the mapped geothermal vegetation types. Points that fell onto tracks and boardwalks were visually removed using the RGB imagery to prevent any anomalies in the datasets. Further points were also removed due to no data being available in either the NDVI or TIR datasets supplied to us. This resulted in a final selection of 9,051 points. We ran these points through the ArcGIS ‘Extract Multi Values to Points’ tool to calculate both the TIR and NDVI at the points. These data were then exported to Microsoft Excel for further analysis.

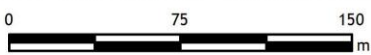


Legend
 Substrate sampling areas

Data Acknowledgment
 Maps contain data sourced from LINZ
 Crown Copyright Reserved

Report: R4010
 Client: ENWWALK
 Ref: 01 1698
 Path: E:\gis\EW_Geothermal_Sites_2003\UAV_data\mxd\
 File: Craters_training.mxd

Figure 3. Substrate sample points for NDVI analysis, Craters of the Moon Geothermal Area



Wildlands
 www.wildlands.co.nz, 0508 WILDNZ

Scale: 1:3,000
 Date: 10/08/2016
 Cartographer: RPB
 Format: A3

3.4.5 Photopoint analysis of Aerial based TIR versus NDVI

Each photopoint was buffered with a five metre radius of the photopoint origin. The TIR and NDVI was then cut to these buffers and then a mean value for both was recorded for each photopoint and exported to Microsoft Excel. These clips ended up as a square based on the extent of the photo and clipped outwards to the nearest cell. Due to the difference in cell size (NDVI = 0.044 m and TIR = 0.169 m) and a different origin this resulted in not querying the exact same area for both values.

3.5 Statistical analyses

Four measures of central tendency were taken for each ground-based photopoint. They were the mean and median across the entire set of NDVI scores, and mean and median NDVI across the photosynthetic range (0.01-0.2, hereafter referred to as PNDVI). Linear regression was used to explore the relationship between these measures of central tendency and vegetation height. Linear regression was also used to explore the relationship between TIR in a 5m radius estimated from drone footage and NDVI derived from ground based photopoints. Density plots using kernel density estimates were used to characterise the distribution of these measures of NDVI central tendency across photopoints within the same vegetation type. All analyses were undertaken in R (R Core Team 2014).

4. STRESS AND GEOTHERMAL VEGETATION

One issue with using NDVI to assess heat-stressed geothermal vegetation is that vegetation at a geothermal site could be suffering from a range of plant stressors such as soil toxicity, lack of nutrients, drought, frost, pathogens, and not just from heat stress. Other stressors may also be involved, such as deliberate or accidental herbicide spraying. In addition, stresses may operate only irregularly, and the agent of stress may be undetectable in a one-off survey (for example the effects of frost are not likely to be detected in summer, and may not be detectable in every winter season). Identifying heat-stressed plants in the naturally stressed geothermal environment, and attributing a simple cause to the stress is therefore problematic. However, having identified areas of stressed vegetation, the cause of the stress can then be investigated by other means.

5. NORMALISED DIFFERENCE VEGETATION INDEX (NDVI)

5.1 Overview

The density of green vegetation over the Earth can be measured and mapped by carefully measuring the wavelengths and intensity of visible and near-infrared light reflected by the land surface. Chlorophyll in plant leaves strongly absorbs visible light (from 0.4 to 0.7 μm) for use in photosynthesis. The cell structure of the leaves, on the other hand, strongly reflects near-infrared light (from 0.7 to 1.1 μm). The greater the leaf density, the more these wavelengths of light are affected. In general, if there is much more reflected radiation in near-infrared wavelengths than in visible wavelengths, then the vegetation is likely to be dense. If there is very little difference

in the intensity of visible and near-infrared wavelengths reflected, then the vegetation is probably sparse. Alternatively, healthy vegetation will absorb most of the visible light that hits it and reflect a large portion of the near-infrared light, while unhealthy vegetation will reflect more visible light and less near-infrared light (Weier and Herring 2000). The reflectivity of plant tissues also changes during the growing season, e.g. from early spring growth to late-season maturity and senescence (U.S. Geological Survey 2015).

The Normalised Difference Vegetation Index (NDVI) is one of several indices used to quantify the density of plant growth on the Earth's surface. Use of the index can compensate for changing illumination conditions, surface slope, and viewing angle (U.S. Geological Survey 2015). NDVI is calculated as:

$$\text{NDVI} = (\text{NIR} - \text{VIS}) / (\text{NIR} + \text{VIS})$$

where NIR is the amount of near-infrared light reflected and VIS is the amount of visible light reflected.

Values of NDVI can range from -1.0 to +1.0, but values less than zero typically do not have any ecological meaning, so the range of the index is often truncated to 0.0 to +1.0. Higher values signify a larger difference between the red and near infrared radiation recorded by the sensor - a condition associated with highly photosynthetically-active vegetation. Low NDVI values mean there is little difference between the red and NIR signals. This happens when there is little photosynthetic activity, or when there is just very little NIR light reflectance (e.g. water reflects very little NIR light).

5.2 Limitations of NDVI

Use of the NDVI has the following limitations/issues:

- The NDVI is correlated with a number of attributes that are of interest to ecologists and managers (e.g. percent cover of bare ground and vegetation, biomass). It is not, however, a direct measure of any of these things - it is a measure of “greenness” produced by the ratio of infrared and red light that is reflected from the surface (The Landscape Toolbox 2013).
- There are a lot of factors that influence the strength of the relationship between NDVI and ecosystem attributes. These can include: atmospheric conditions, scale of the imagery, vegetation moisture, soil moisture, overall vegetative cover, and differences in soil type. It is important when using NDVI data in analyses that steps be taken to understand and, to the extent possible, control for factors that might be affecting NDVI values before interpretations of differences in NDVI between areas of within the same area over time can be made (The Landscape Toolbox 2013).
- Light from the soil surface can influence the NDVI values by a large degree. Soils tend to darken when wet, so that their reflectance is a direct function of water content. If the spectral response to moistening is not exactly the same in the two spectral bands, the NDVI of an area can appear to change as a result of soil moisture changes (precipitation or evaporation) and not because of vegetation

changes (Wikipedia 2016). This is of concern in habitats with a higher cover of bare ground and exposed rock. Heute and Jackson (1988) found that the soil surface impact on NDVI values was greatest in areas with between 45% and 70% vegetative cover. This limitation was the reason for the development of the several different soil-adjusted vegetation indices (e.g. Soil-adjusted Vegetation Index, Modified Soil-adjusted Vegetation Index) (The Landscape Toolbox 2013).

- There is a loss of sensitivity to changes in amount of vegetation at the high-cover/biomass end of the scale. This means that as the amount of green vegetation increases, the change in NDVI gets smaller and smaller. So at very high NDVI values, a small change in NDVI may actually represent a very large change in vegetation. This type of sensitivity change is problematic for analysis of areas with a high amount of photosynthetically active vegetation. In these situations, it may be advisable to use another vegetation index with better sensitivity to high-vegetation cover situations such as the Enhanced Vegetation Index or the Wide Dynamic Range Vegetation Index (The Landscape Toolbox 2013).
- While dividing through by NIR+VIS may have been an excellent normalisation factor for comparing large swaths of earth illuminated uniformly, a small denominator can unduly influence the vegetation index. Practically, this means something of low visible and NIR reflectance will paradoxically produce a very strong NDVI signal. For example, the shadows cast by crops on a small scale and clouds on a larger scale dramatically affect these images (Agribotix 2014).
- The NDVI signal can vary wildly over time due to changes in reflectivity through the plant growth cycle (Agribotix 2014).
- Comparisons between sites are very difficult due to the NDVI signal varying with plant health, incident light, time of year, and stage in plant development (Agribotix 2014).

5.3 NDVI values used to assess vegetation

NDVI ranges from -1.0 to +1.0. Areas of barren rock, sand, standing water, or snow usually show very low NDVI values (for example, 0.1 or less). Sparse vegetation such as shrubs and grasslands or senescing crops may result in moderate NDVI values (approximately 0.2 to 0.5). High NDVI values (approximately 0.6 to 0.9) correspond to dense vegetation such as that found in temperate and tropical forests or crops at their peak growth stage (U.S. Geological Survey 2015).

6. RESULTS

Twenty-seven photopoints, taken from a downwards facing position, were available for analysis. These were spread across a large number of habitats with the largest sample being in geothermal kanuka scrub (15 photos). Most other habitat types only had one photograph (Table 3). Photos were taken within a narrow timeframe (days) at similar time of day, and under similar weather conditions, limiting seasonal, weather, or other time dependent changes. All changes should be space related, or maturity related.

Table 3: Geothermal habitats sampled by the 27 photopoints.

HabitatType	Number of Photographs
Baygrass/bare ground grassland	1
Bracken fernland	1
<i>Campylopus</i> spp mossfield	4
<i>Cotoneaster glaucophyllus</i> scrub	1
Geothermal kānuka scrub	15
Geothermal kānuka shrubland	1
<i>Lycopodiella cernua</i> fernland	1
Mingimingi scrub	2
Ratstail grassland	1

6.1 Ground-based NDVI analyses

6.1.1 Ground-based NDVI and vegetation dieback

Out of the four measures of NDVI central tendency (mean NDVI, median NDVI, mean PNDVI, median PNDVI) median NDVI correlated most strongly with vegetation dieback (Figure 4) with an adjusted $R^2=0.38$ ($F=16.7$, d.f.=1,25, $p=0.0003964$), compared with 0.31 for mean NDVI, 0.28 for median PNDV, and 0.25 for mean PNDVI. However, regression diagnostics indicated some high leverage values and that residual variance was not always homogenous.

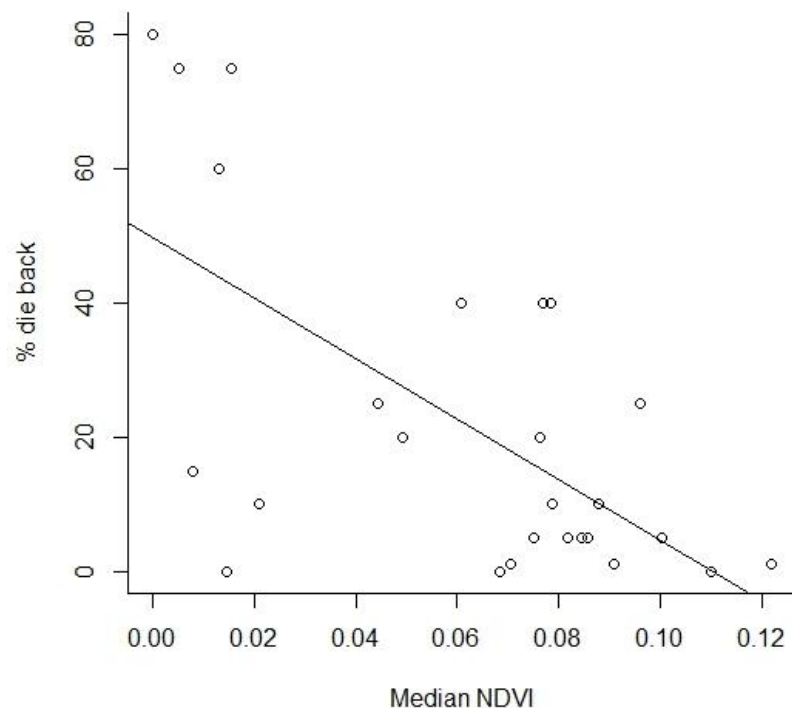


Figure 4: The relationship between percentage dieback and median NDVI.

The correlation between median NDVI and percentage dieback becomes much stronger, and the assumptions of linear regression are met, if geothermal kanuka scrub is considered on its own ($F=76.84$, $df=1,12$, $adj-R^2=0.85$, $p=0.000001$; Figure 5).

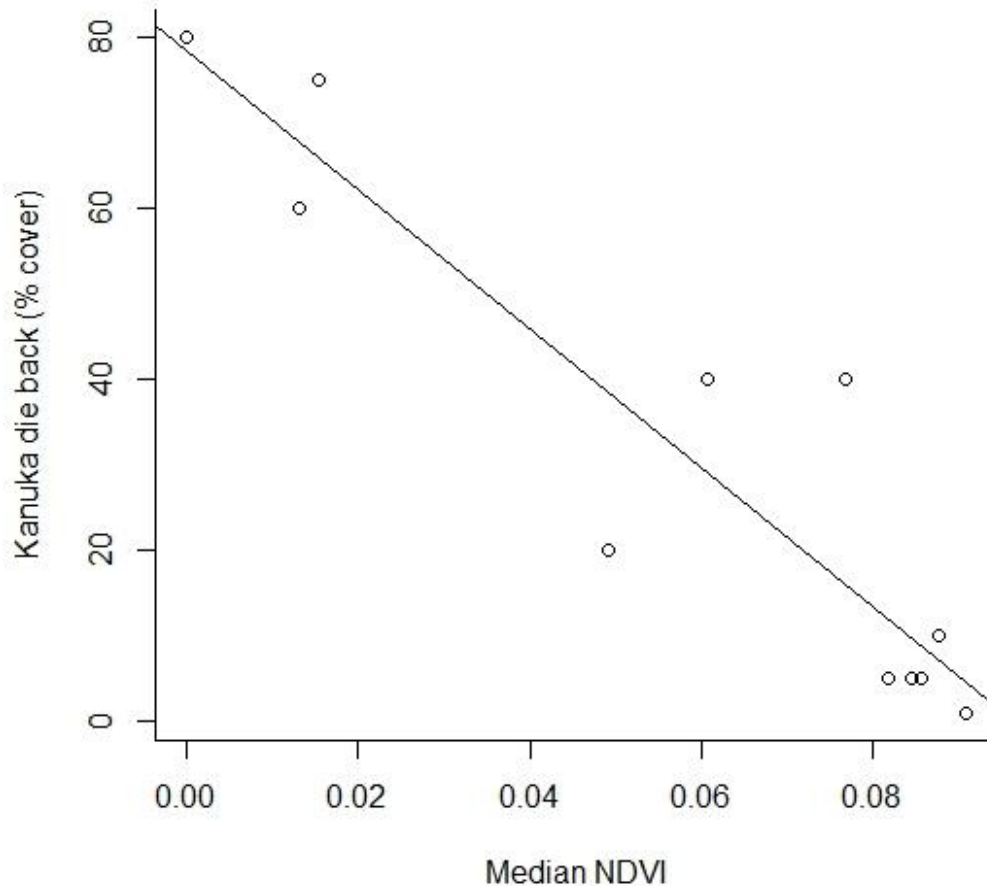


Figure 5: The correlation between geothermal kanuka scrub dieback and median ground-based NDVI (adj-R²=0.85).

6.1.2 Ground-based NDVI and vegetation height

As with the dieback analysis, analysis of vegetation height was stronger if geothermal kanuka scrub was considered on its own. There were strong correlations between geothermal kanuka scrub and the various measures of NDVI central tendency. However, demonstrating these correlations required the elimination of one outlier that had a very high NDVI value associated with a geothermal kanuka height of 135 cm (Figure 6). When this outlier was removed mean NDVI had the strongest correlation with geothermal kanuka scrub height with an adjusted R² of 0.51 ($F=14.29$, d.f.=1,12, $p=0.003$; Figure 7), compared with an adjusted R² of 0.50 for median NDVI, 0.42 for median PNDVI, and 0.40 for mean PNDVI.

6.1.1 Ground-based NDVI and habitat type

Of the vegetation types identified in Table 2 only geothermal kanuka scrub had sufficient data to attempt to characterise the distribution of NDVI values for that vegetation type. Figures 8 and 9 show that median and mean NDVI scores for the fifteen geothermal kanuka scrub photographs were typically in the 0.05-0.12 range.

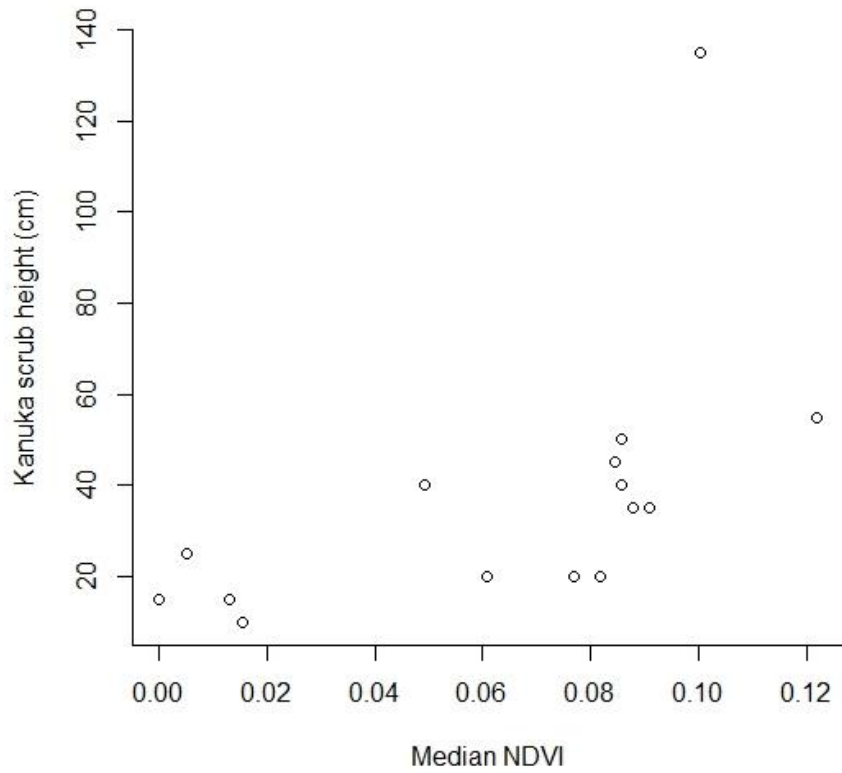


Figure 6: Scatterplot of geothermal kanuka scrub height and median NDVI demonstrating an obvious outlier (135 cm high geothermal kanuka with a median NDVI of 0.11).

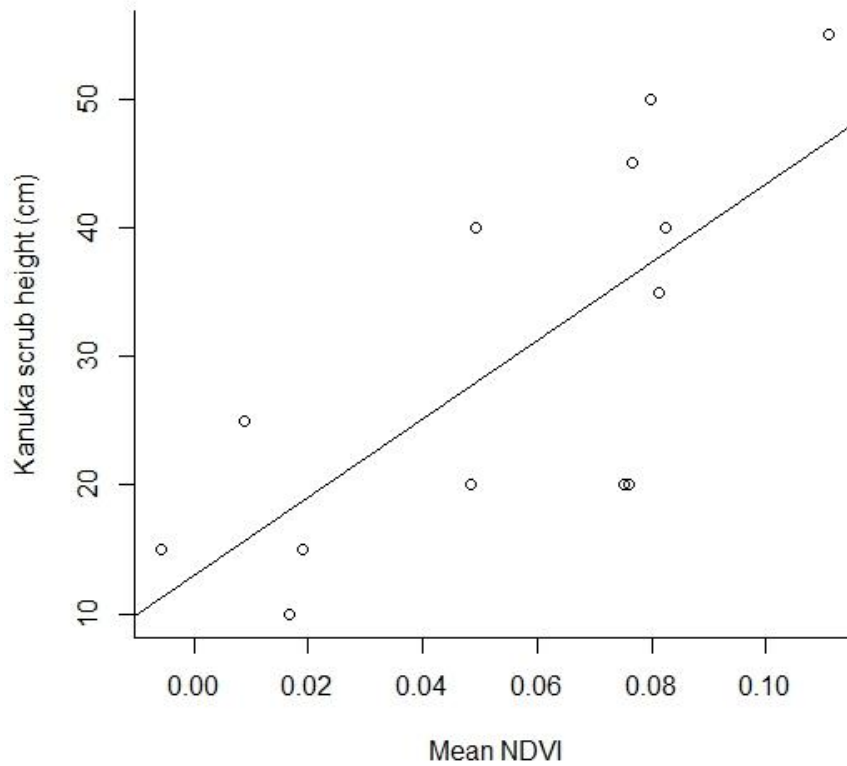


Figure 7: The relationship between mean NDVI and geothermal kanuka scrub height (adjusted $R^2=0.51$).

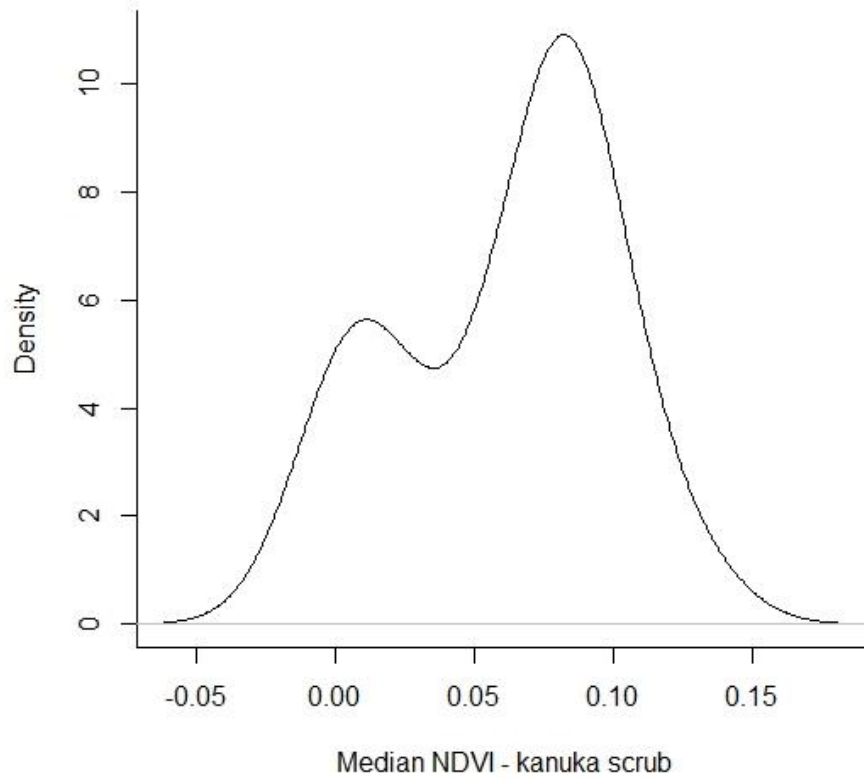


Figure 8: Density function showing the distribution of median NDVI values across 15 photopoints for geothermal kanuka scrub.

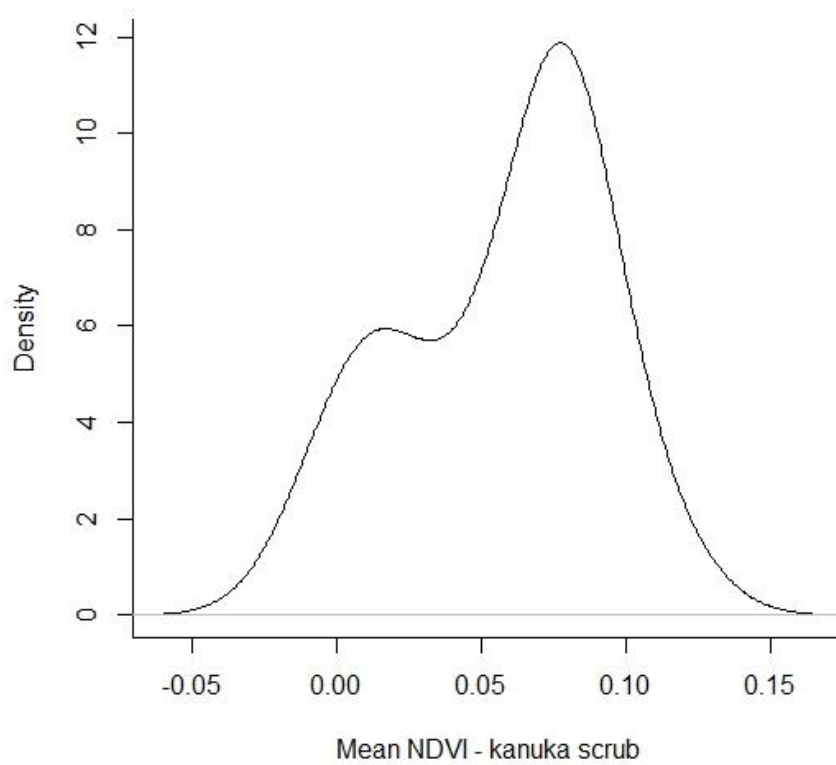


Figure 9: Density function showing the distribution of mean NDVI values across 15 photopoints for geothermal kanuka scrub.

6.2 Aerial TIR and NDVI analyses

6.2.1 Aerial TIR versus aerial NDVI in geothermal kanuka

Mean aerial TIR values from five metres radii around photopoint sites were regressed against median aerial NDVI values from photopoints of geothermal kanuka scrub. The regression demonstrated a negative correlation between TIR and NDVI ($F=11.58$, $df=1,13$, $adj-R^2=0.43$, $p=0047$). However, three outlying values were found to have significant leverage on the regression (Figure 10), and we were unable to identify reasons for their exclusion. Therefore we recommend that this result be treated cautiously, and that the relationship between TIR and NDVI needs to be evaluated more thoroughly with a larger dataset.

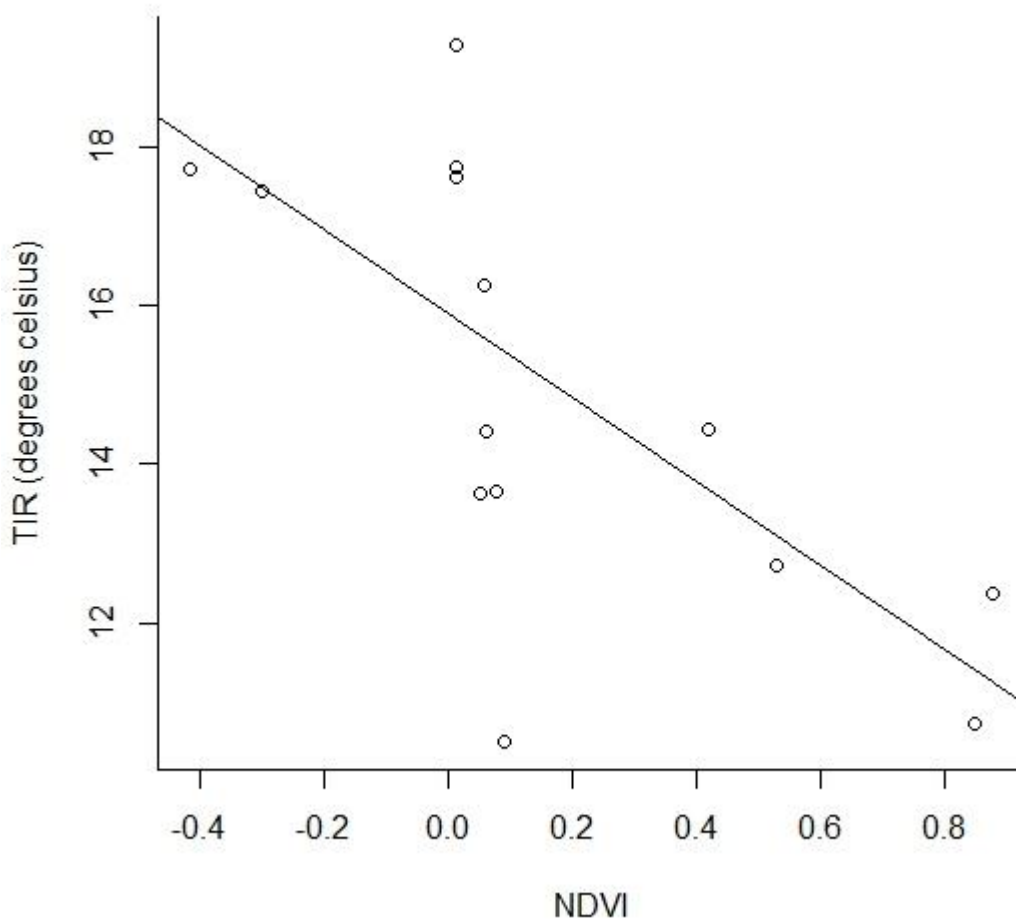


Figure 10: The relationship between TIR and median NDVI values from drone imagery in a 5m radius of where photopoints were taken within geothermal kanuka scrub.

6.2.2 Aerial TIR versus aerial NDVI for geothermal habitats

Aerial TIR and NDVI values derived from sampling of the drone-collected imagery across the entire Craters of the Moon site were plotted against each other. In general the relationship is negative and would likely be significant, but the amount of scatter would result in a low R^2 value (Figure 11).

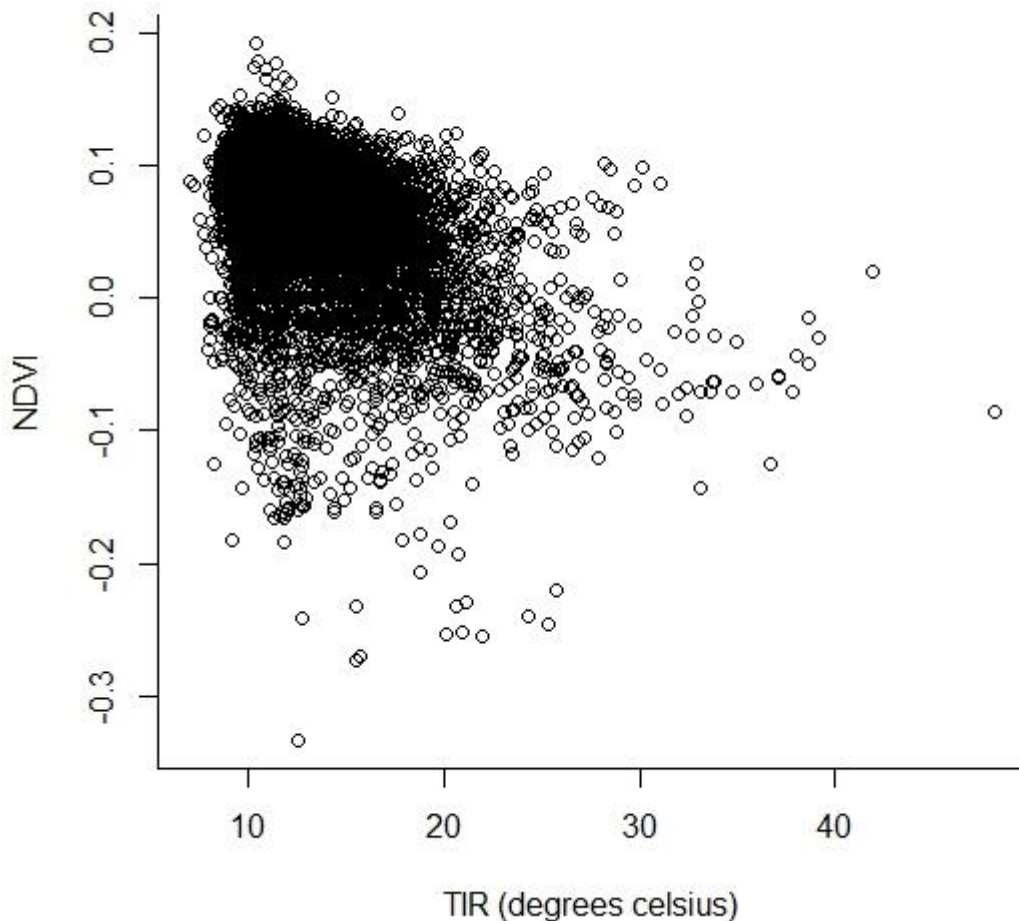


Figure 11: The relationship between TIR and NDVI values from drone imagery for geothermal vegetation and habitat at Craters of the Moon.

6.2.1 Aerial TIR versus geothermal stress and ground-based NDVI

Aerial TIR was not related to geothermal kānuka dieback ($F=0.007, df=1,10, R^2=-0.1, p=0.94$), geothermal kānuka height ($F=0.09, df=1,10, R^2=-0.09, p=0.77$), or median. ($F=0.61, df=1,2, R^2=-0.02, p=0.44$) or mean ($F=0.15, df=1,2, R^2=-0.04, p=0.70$) values for ground-based NDVI (Figure 12).

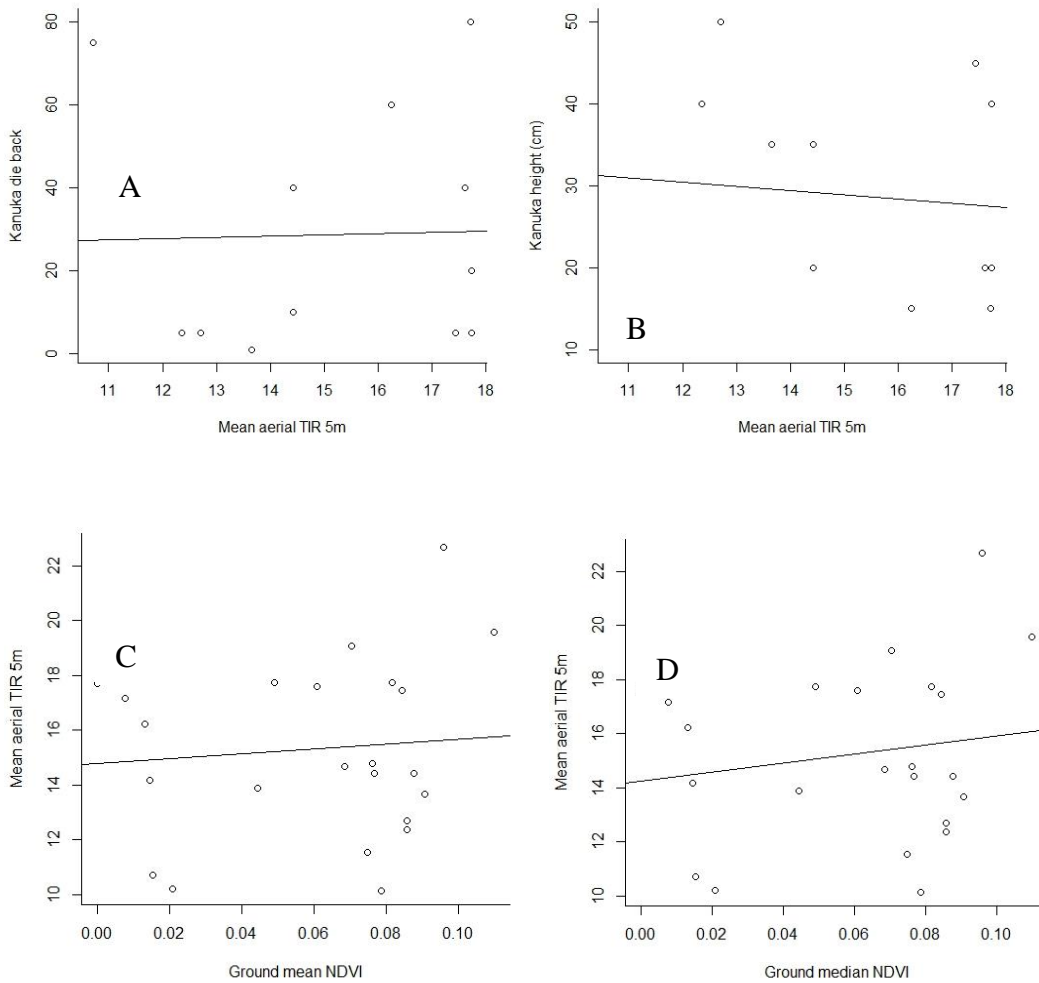


Figure 12: Relationships between aerial TIR and (a) geothermal kākūka dieback (b) geothermal kākūka height (c) mean ground-based NDVI and (d) median ground based NDVI at Craters of the Moon.

6.3 Soil temperature and geothermal vegetation stress

6.3.1 Soil temperature and geothermal kākūka dieback

Relationships between soil temperature at different depths and geothermal kākūka dieback all had positive slopes, but also had considerable scatter (Figure 13), and consequently had very low R^2 values. None of these relationships were statistically significant, with soil temperature at 40 cm depth having the lowest p -value of 0.24.

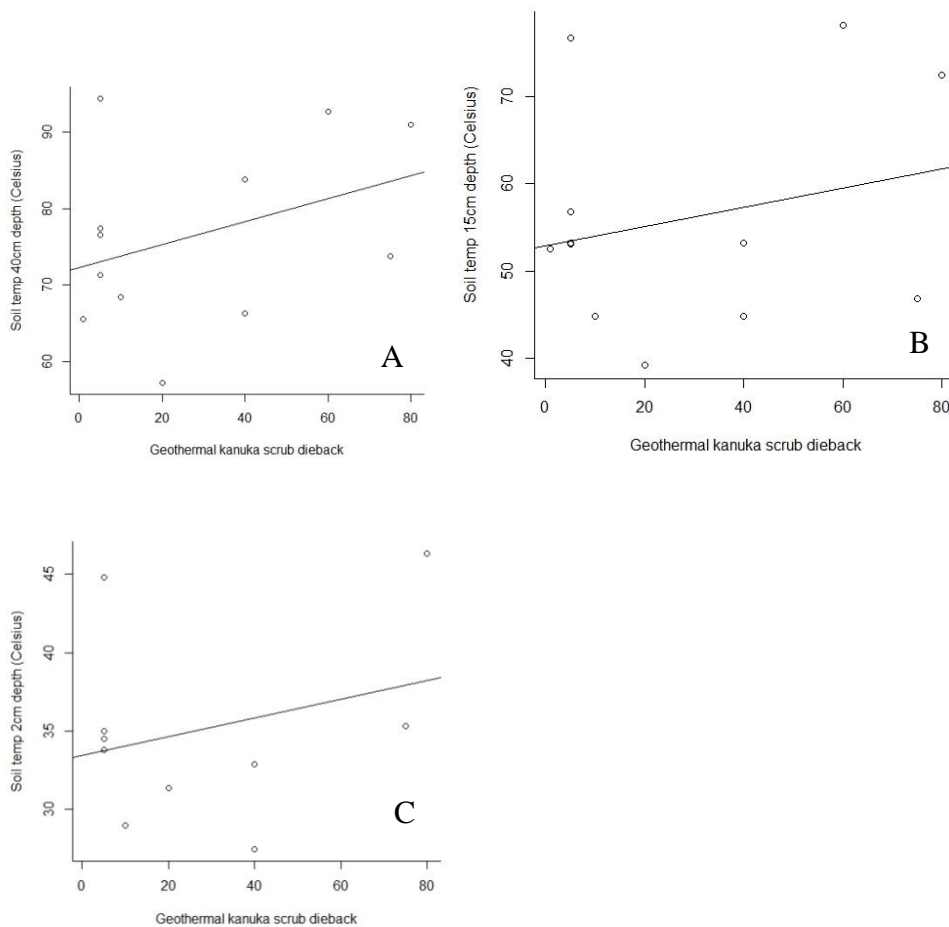


Figure 13: Relationships between geothermal kānuka dieback and (a) soil temperature at 40 cm depth (b) soil temperature at 15 cm depth (c) soil temperature at 2 cm depth.

6.3.2 Soil temperature and geothermal kānuka height

As with geothermal kānuka dieback, soil temperature was not related to geothermal kānuka height, at any of the three levels that soil temperature was measured (Figure 14). The slope of the relationship was negative at all three soil temperatures, but R^2 values were again very low, and the lowest p -value of 0.32 was observed when soil temperature at 2 cm depth was related to geothermal kānuka height.

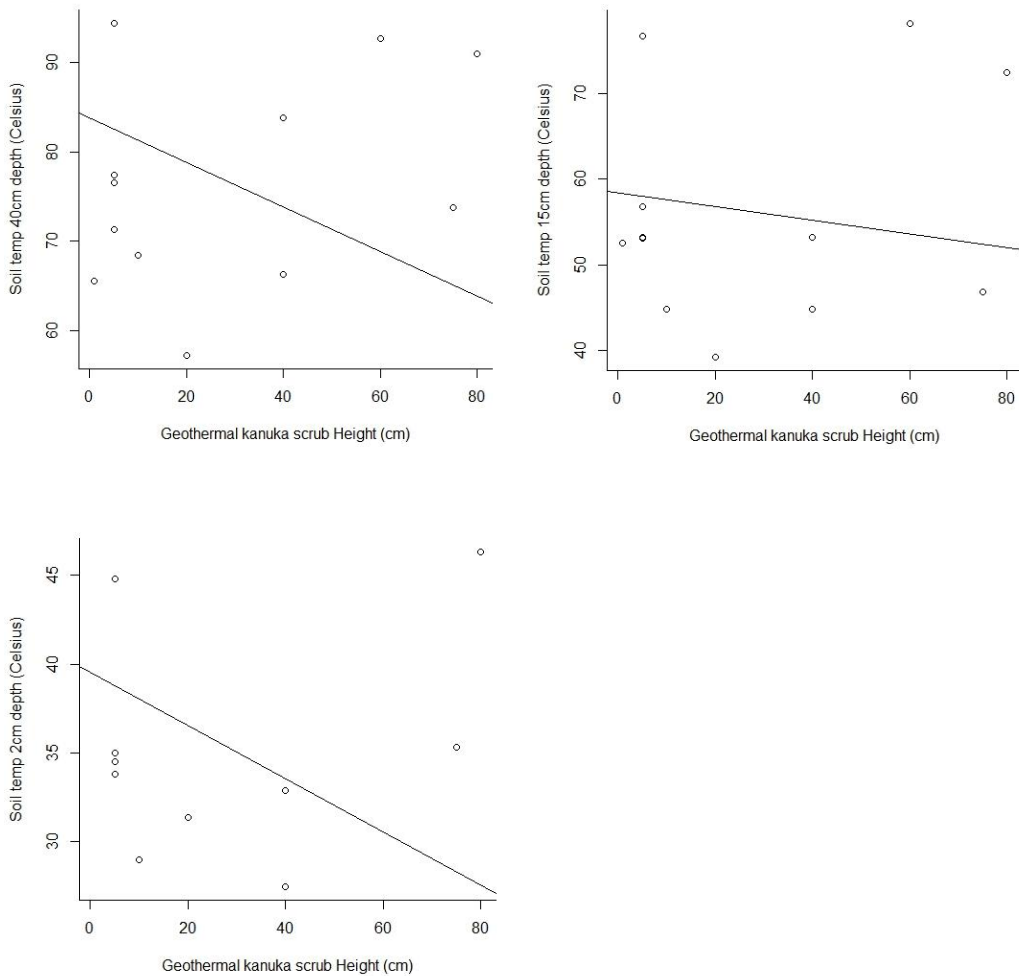


Figure 14: Relationships between geothermal kānuka dieback and (a) soil temperature at 40 cm depth (b) soil temperature at 15 cm depth (c) soil temperature at 2 cm depth.

7. DISCUSSION

We observed significant relationships between several of the variates assessed in our analyses. Ground-based NDVI was negatively related to geothermal kānuka dieback, and positively related to geothermal kānuka height. When summarising NDVI values from photopoints we recommend using median NDVI because the distribution of NDVI values is typically skewed.

Geothermal habitats had relatively low NDVI compared to published values. Geothermal kānuka generally has an NDVI value within the 0.05-0.12 range. Other habitat types were not sampled sufficiently to establish their typical NDVI ranges. The season of sampling (late autumn, early winter) may have influenced the relatively low NDVI values observed at the Craters of the Moon site. Sampling in the growing season (spring and summer) could provide potentially different interpretations.

In order to regress ground-based NDVI against the height of geothermal kanuka scrub we had to remove an outlier. The outlying observation was for geothermal kanuka scrub with a height of 135 cm. We recommend further evaluation of the relationship between NDVI and geothermal scrub in the 60 cm-135 cm range to determine whether this is a legitimate outlier or whether there is a curvilinear relationship between NDVI and geothermal kanuka scrub height.

Overall NDVI was a much better predictor of geothermal kanuka scrub height and dieback than NDVI values from the photosynthetic range (0.01-0.2). This is most likely because NDVI values from the photosynthetic range would not include dead material, or bare ground visible beneath low-stature geothermal kākūka, which are characteristic features of more stressed geothermal vegetation types.

We did not make an assessment of whether there was spatial independence between the various photopoints we used in this analysis; rather, we were simply interested in whether NDVI related to these different variables at the scale we measured them at in order to determine whether NDVI could be used to predict these variables.

Although there appears to be a correlation between aerial TIR and aerial NDVI the sample size was small and three large outliers suggest that this relationship should be more carefully evaluated with a larger dataset. A sampling approach relating aerial TIR and ground-based NDVI produced considerable scatter but showed a general negative relationship between these two variates.

Aerial TIR at ground-based photography sites had no relationship with geothermal kākūka dieback or height. Aerial TIR was also not related to mean or median ground-based NDVI. Similarly, soil temperatures at photograph sites were not significantly associated with kākūka dieback or height.

8. CONCLUSIONS

Stressed geothermal vegetation (identified subjectively through percentage cover of dead foliage), and in particular vegetation dominated by geothermal kākūka, can be identified by ground-based NDVI values at a relatively small scale. This suggests that aerial NDVI may also be able to determine geothermal vegetation stress. There was a strong relationship between stressed geothermal kākūka and median ground-based NDVI. Ground-based NDVI was also strongly related to geothermal kākūka height, so long as an outlying value was removed. The cause of the stress may not, however, be heat flow within the ground, or if heat flow is involved it may be interacting with other factors. NDVI and TIR derived from drone-collected imagery have a broadly negative relationship, implying that at higher temperatures leaf density is lower, but this relationship requires further analysis using a larger dataset to establish its true pattern. Aerial TIR had a surprisingly poor relationship with geothermal kākūka dieback or stature, and was also poorly related to ground-based NDVI. Furthermore, soil temperatures at three different depths were not significantly associated with geothermal kākūka dieback or height. Thus we were unable to determine whether changes in heat flow are responsible for stress-effects on geothermal vegetation and habitat. Further work is required to validate the relationship between geothermal kākūka height and NDVI, and the relationship between TIR and NDVI. These

conclusions are also limited through being interpreted from data collected from just one geothermal site, and at one time of year.

ACKNOWLEDGMENTS

We would like to thank Katherine Luketina and Jim McLeod (Waikato Regional Council) for instigating this project. The Craters of the Moon Trust kindly provided access permission for work at the site.

REFERENCES

- Agribotix 2014: Misconceptions about UAV-collected NDVI imagery and the Agribotix experience in ground truthing these images for agriculture. <http://agribotix.com/blog/2014/06/10/misconceptions-about-uav-collected-ndvi-imagery-and-the-agribotix-experience-in-ground-truthing-these-images-for-agriculture/>.
- Blue Marble Research 2003: NDVI Measurements with Simple Radiometric and photographic Methods. Estimating NDVI using Infrared Photography. <http://bluemarble.ch/wordpress/2003/01/07/ndvi-measurements-with-simple-radiometric-and-photographic-methods/>.
- Harvey M.C., Rowland J.V., and Luketina K.M. 2016: Drone with thermal infrared camera provides high resolution georeferenced imagery of the Waikite geothermal area, New Zealand. *Journal of Volcanology and Geothermal Research* 325: 61-69.
- Holben B.N. 1986: Characteristics of Maximum-Value Composite Images from Temporal AVHRR Data. *International Journal of Remote Sensing* 7(11): 1417-1434.
- Huete A.R. and Jackson R.D. 1988: Soil and atmosphere influences on the spectra of partial canopies. *Remote Sensing of the Environment* 25:89-105.
- R Core Team 2014: R: A language and environment for statistical computing. R Foundation for Statistical Computing, Vienna, Austria. URL <http://www.R-project.org/>.
- Soudani K., Hmimina G., Delpierre N., Pontailier J.-Y., Aubinet M., Bonal D., Caquet B., de Grandcourt A., Burban B., Flechard C., Guyon D., Granier A., Gross P., Heinesh B., Longdoz B., Loustau D., Moureaux C., Ourcival J.-M., Rambal S., Saint André L., and Dufrêne E. 2012: Ground-based Network of NDVI measurements for tracking temporal dynamics of canopy structure and vegetation phenology in different biomes. *Remote Sensing of Environment* 123: 234-245.
- The Landscape Toolbox 2013: Normalised Difference Vegetation Index. http://wiki.landscapetoolbox.org/doku.php/remote_sensing_methods:normalised_difference_vegetation_index.
- U.S. Geological Survey 2015: NDVI, the Foundation for Remote Sensing Phenology. http://phenology.cr.usgs.gov/ndvi_foundation.php.

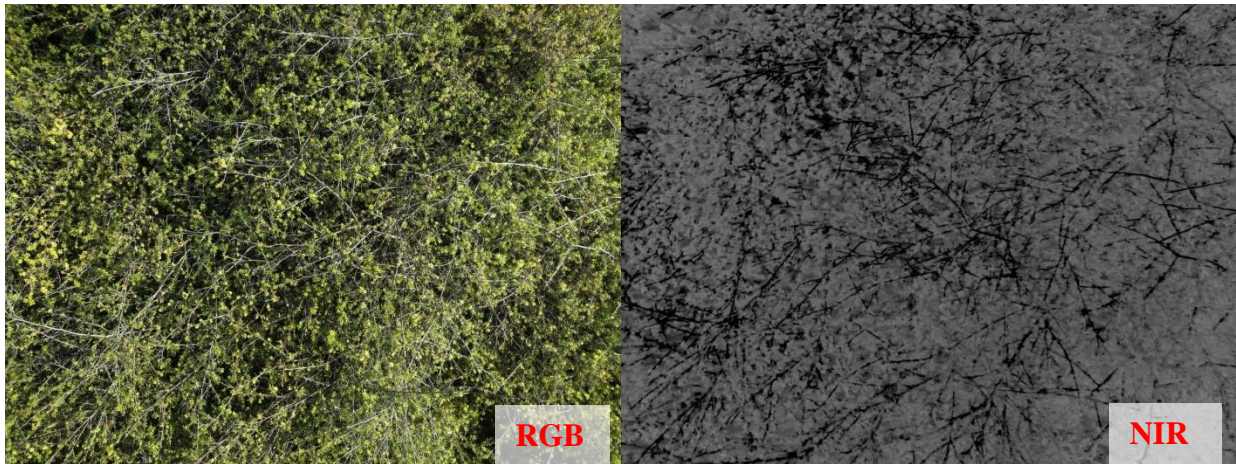
Weier J. and Herring D. 2000: Measuring vegetation (NVDI and EVI). <http://earthobservatory.nasa.gov/Features/MeasuringVegetation/>.

Wikipedia 2016: Normalised Difference Vegetation Index. *Wikipedia, The Free Encyclopaedia*. https://en.wikipedia.org/wiki/Normalized_Difference_Vegetation_Index.

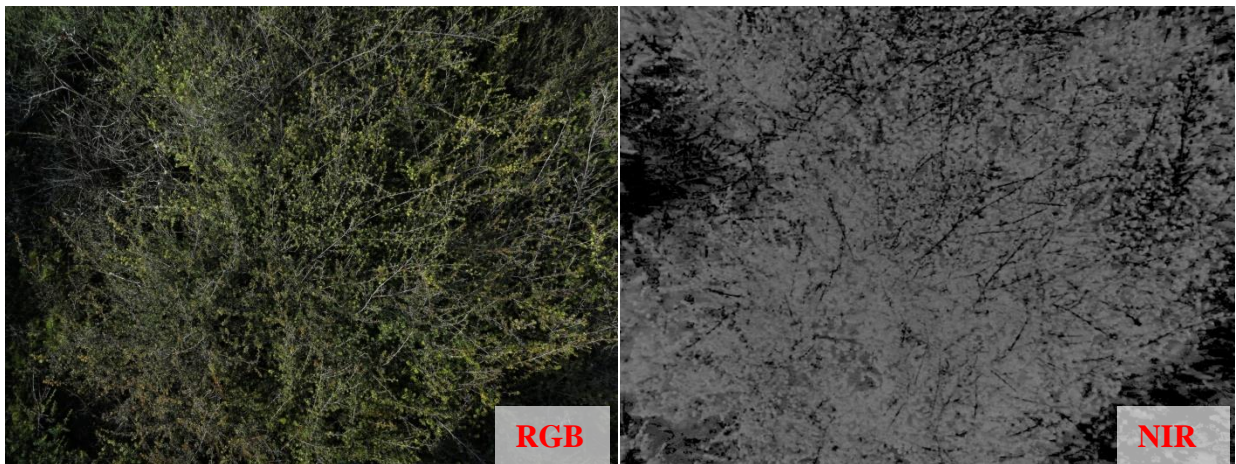
Wildland Consultants 2014: Geothermal vegetation of the Waikato Region, 2014. *Wildland Consultants Ltd Contract Report No. 3330*. Prepared for Waikato Regional Council. 538 pp.

GROUND-BASED VERTICAL RGB AND NIR PHOTOGRAPHS

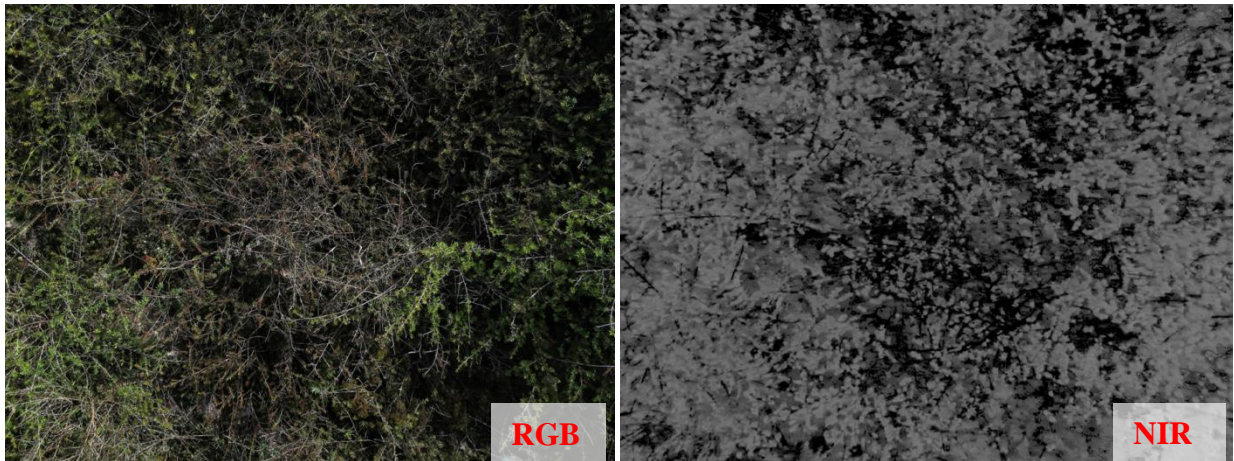
Site 4: Healthy geothermal kānuka, 0.5 m tall, with 5% dieback. Temperature at different soil depths: 2cm 35°C; 15cm 57°C; 40cm 71°C



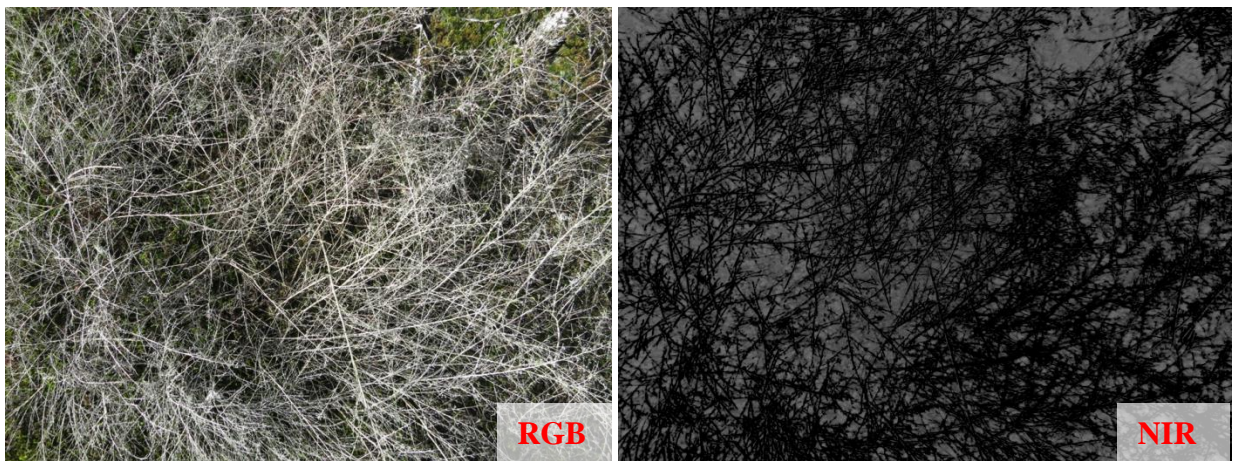
Site 3: Healthy geothermal kānuka, 0.35 m tall, with 10% dieback. Temperature at different soil depths: 2cm 29°C; 15cm 45°C; 40cm 68°C



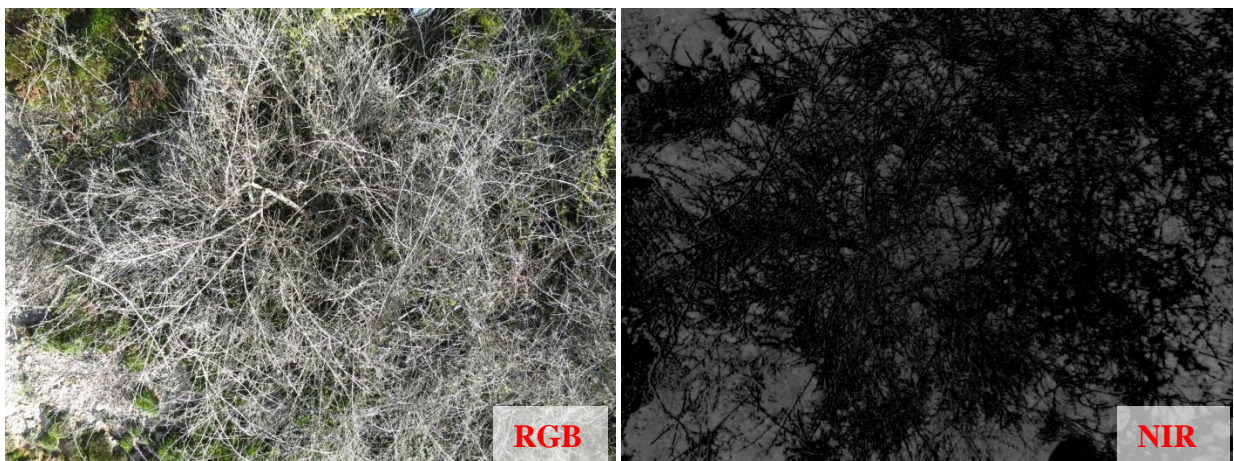
Site 5: Moderately healthy geothermal kānuka, 0.15 m tall, with 40% dieback. Temperature at different soil depths: 2cm 33°C; 15cm 53°C; 40cm 84°C



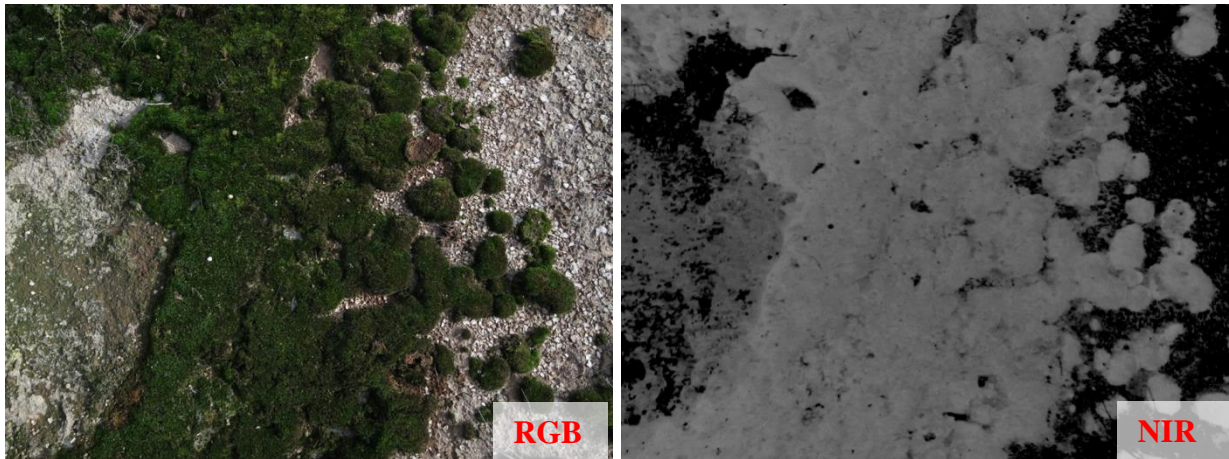
Site 14: Mostly dead geothermal kānuka, 0.1 m tall, with 10% live kānuka, and 75% bryophyte cover. Temperature at different soil depths: 2cm 35°C; 15cm 47°C; 40cm 74°C



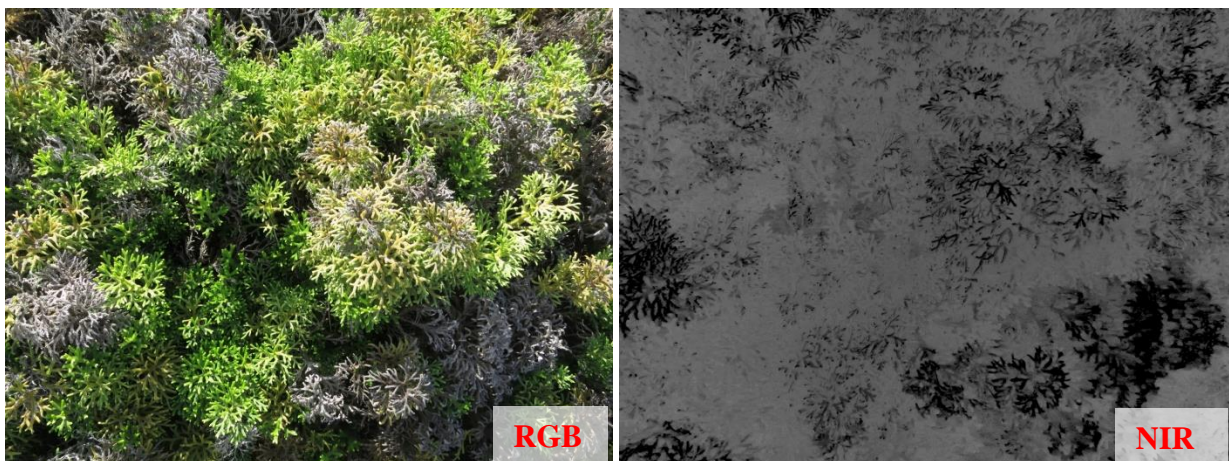
Site 7: Dead geothermal kānuka, 0.25 m tall, with 75% dead kānuka, and 40% bryophyte cover. Temperature at different soil depths: 2cm 45°C; 15cm 54°C; 40cm 77°C



Site 6: Mossfield, 0.02 m tall, with 80% bryophyte cover. Temperature at different soil depths: 2cm 33°C; 15cm 47°C; 40cm 83°C



Site 16: *Lycopodiella cernua* fernland, 0.5 m tall, with 25% dead foliage. Temperature at different soil depths: 2cm 24°C; 15cm 25°C; 40cm 27°C





Wildlands

*Providing outstanding ecological services
to sustain and improve our environments*

Call Free 0508 WILDNZ
Ph: +64 7 343 9017
Fax: +64 7 3439018
ecology@wildlands.co.nz

99 Sala Street
PO Box 7137, Te Ngae
Rotorua 3042,
New Zealand

Regional Offices located in
Auckland, Hamilton, Tauranga,
Whakatane, Wellington,
Christchurch and Dunedin

ECOLOGY RESTORATION BIODIVERSITY SUSTAINABILITY

www.wildlands.co.nz